

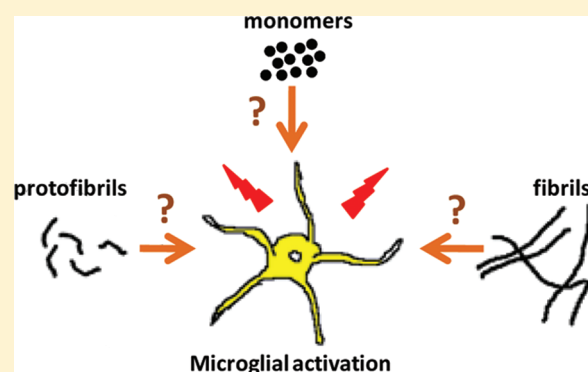
Isolated Amyloid- β (1–42) Protofibrils, But Not Isolated Fibrils, Are Robust Stimulators of Microglia

Geeta S. Paranjape, Lisa K. Gouwens, David C. Osborn, and Michael R. Nichols*

Department of Chemistry and Biochemistry and Center for Nanoscience, University of Missouri—St. Louis, St. Louis, Missouri 63121, United States

ABSTRACT: Senile plaques composed of amyloid- β protein ($A\beta$) are an unshakable feature of the Alzheimer's disease (AD) brain. Although there is significant debate on the role of the plaques in AD progression, there is little disagreement on their role in stimulating a robust inflammatory response within the context of the disease. Significant inflammatory markers such as activated microglia and cytokines are observed almost exclusively surrounding the plaques. However, recent evidence suggests that the plaque exterior may contain a measurable level of soluble $A\beta$ aggregates. The observations that microglia activation in vivo is selectively stimulated by distinct $A\beta$ deposits led us to examine what specific form of $A\beta$ is the most effective proinflammatory mediator in vitro. We report here that soluble prefibrillar species of $A\beta$ (1–42) were better than fibrils at inducing microglial tumor necrosis factor α (TNF α) production in either BV-2 and primary murine microglia. Reconstitution of $A\beta$ (1–42) in NaOH followed by dilution into F-12 media and isolation with size exclusion chromatography (SEC) revealed classic curvilinear β -sheet protofibrils 100 nm in length. The protofibrils, but not monomers, markedly activated BV-2 microglia. Comparisons were also made between freshly isolated protofibrils and $A\beta$ (1–42) fibrils prepared from SEC-purified monomer. Surprisingly, while isolated fibrils had a much higher level of thioflavin T fluorescence per mole, they were not effective at stimulating either primary or BV-2 murine microglia compared to protofibrils. Furthermore, SEC-isolated $A\beta$ (1–40) protofibrils exhibited significantly less activity than concentration-matched $A\beta$ (1–42). This report is the first to demonstrate microglial activation by SEC-purified protofibrils, and the overall findings indicate that small, soluble $A\beta$ (1–42) protofibrils induce much greater microglial activation than mature insoluble fibrils.

KEYWORDS: Alzheimer's disease, inflammation, amyloid-beta protein, tumor necrosis factor alpha, protofibrils, fibrils



Alzheimer's disease (AD) is a complex neurodegenerative disease characterized by the accumulation of protein deposits in the affected brain and progressive dementia. The two classic forms of deposits are neurofibrillary tangles composed of tau protein and dense core neuritic plaques composed of amyloid- β protein ($A\beta$).¹ Both lesions are believed to contribute to disease onset and progression although the initial event appears to be $A\beta$ accumulation.² $A\beta$ is commonly produced as an unstructured 40- or 42-residue peptide fragment by proteolytic cleavage of the amyloid- β precursor protein.³ The monomeric form of $A\beta$ circulates ubiquitously in plasma and cerebrospinal fluid yet an aggregated fibrillar form comprises the characteristic $A\beta$ plaques.¹ The mechanistic complexity of AD is increased by the growing number of reports demonstrating a variety of $A\beta$ structures morphologically distinct from plaques that possess greater solubility and neuronal toxicity.⁴

It has been well documented that inflammatory markers such as activated microglia^{5,6} stained with proinflammatory cytokines⁷ have been observed surrounding the neuritic $A\beta$ plaques in the human AD brain. In fact, studies in an AD transgenic mouse model have shown rapid microglial accumulation around newly formed plaques.⁶ A chronic inflammatory state induced by

accumulated $A\beta$ has been suggested as one of the underlying mechanisms of progressive neurodegeneration in AD⁸ and may in fact exacerbate $A\beta$ deposition.⁹ Multiple studies suggest that small $A\beta$ (1–42) oligomers may cause early and significant alterations in synaptic function and then as fibrillar structures are produced, concomitant inflammatory responses appear (reviewed in ref 4).

In vitro $A\beta$ aggregation studies have contributed significantly to the understanding of fibrillogenesis mechanisms and the structural properties of monomers, soluble intermediates, and mature fibrils. These studies have identified a continuum of $A\beta$ species in the assembly process which vary in their size, length, solubility, and morphology.^{10–14} In solution, $A\beta$ monomers will undergo noncovalent self-assembly¹⁵ to form soluble oligomers,¹⁶ protofibrils¹² that are enriched in β -sheet structure,¹³ and insoluble fibrils.¹⁷ The types of intermediates formed during fibrillogenesis are dependent on the solution conditions.^{12,16}

Received: December 8, 2011

Accepted: January 9, 2012

Published: January 9, 2012

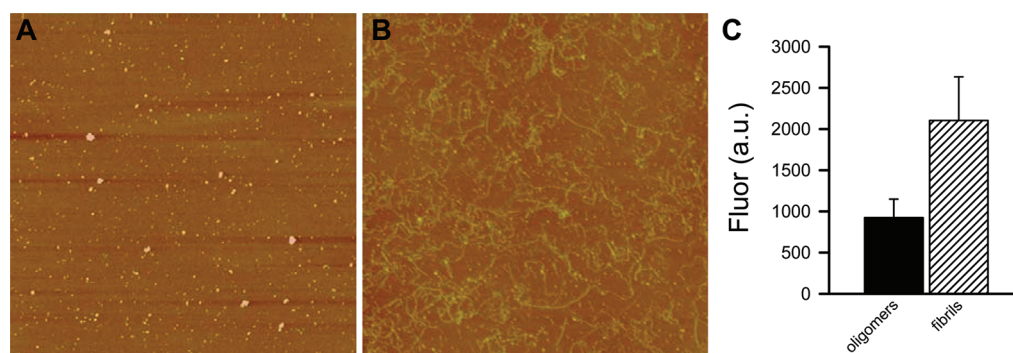


Figure 1. $A\beta(1-42)$ structures formed in oligomer- or fibril-forming conditions are morphologically distinct. Aliquots of lyophilized $A\beta(1-42)$ were reconstituted to $100\ \mu\text{M}$ as described in the Methods to generate oligomers or fibrils. After 24 h incubation at the given temperatures, aliquots of the solutions were diluted to $10\ \mu\text{M}$, applied to mica, and imaged by AFM. Representative images are shown for oligomers (panel A, $5\ \mu\text{m} \times 5\ \mu\text{m}$) and fibrils (panel B, $10\ \mu\text{m} \times 10\ \mu\text{m}$). ThT fluorescence measurements ($n = 8$ for oligomers and $n = 10$ for fibrils) were obtained for each preparation at a final concentration of $10\ \mu\text{M}$ $A\beta(1-42)$ (Panel C).

In addition to significant $A\beta$ polymorphism exhibited in the AD brain, the structural diversity may even extend to the $A\beta$ senile plaques based on recent observations indicating a significant level of oligomeric $A\beta$ surrounding the plaques in an AD mouse model.¹⁸

In concert with in vitro aggregation studies, cellular studies have shown that monomeric, oligomeric, protofibrillar, fibrillar, and amorphous $A\beta$ species possess distinct toxic and biological activities and potencies.^{16,19–22} This is also the case with $A\beta$ as a proinflammatory stimulus. It is generally felt that soluble $A\beta$ oligomers and protofibrils contribute to early dendritic and synaptic injury in AD models (reviewed in ref 23) while fibrillar $A\beta$ acts as a proinflammatory stimulus. However, many groups have reported induction of proinflammatory cytokines and signaling pathways by soluble prefibrillar species in glial cells. In some cases, the type and extent of proinflammatory response differed between $A\beta$ fibrils and soluble oligomeric species.^{24,25} The prevailing view is still that while small soluble $A\beta$ species display greater cellular toxicity, fibrillar structures are the primary mediators of inflammation. Our own studies have indicated that soluble $A\beta(1-42)$ fibrillar precursors were much more effective than fibrils at stimulating tumor necrosis factor α (TNF α) production in human monocytes.²⁶ In many reports, $A\beta$ solutions were used that likely contained a high degree of polydispersity with respect to size and aggregation state. In this study, multiple aggregation conditions were evaluated in conjunction with separation and rigorous characterization of the isolates in order to identify the optimal $A\beta$ species for microglia activation.

RESULTS AND DISCUSSION

Microglial TNF α Production Induced by $A\beta(1-42)$ Prepared in Oligomer-Forming and Fibril-Forming Conditions. LaDu and colleagues previously compared the inflammatory response in rat astrocyte cultures induced by $A\beta$ incubated in oligomer- or fibril-forming conditions.²⁵ We utilized their preparation methods and conditions to prepare $A\beta(1-42)$ solutions that contain species of distinct morphology for evaluation of the inflammatory response in isolated murine microglia. The preparation of the $A\beta$ species entailed reconstitution in DMSO followed by dilution into either cold F12 media (oligomer-forming) or 10 mM HCl (fibril-forming). A 24 h incubation of the $A\beta(1-42)$ solutions at either $4\ ^\circ\text{C}$ (oligomer-forming) or $37\ ^\circ\text{C}$ (fibril-forming) produced the anticipated morphologies for both conditions as assessed by

atomic force microscopy (AFM) (Figure 1A). The images were similar to those of Stine et al.¹⁴ Small punctate globular species were observed in the oligomer preparations (heights $3.1 \pm 1.2\ \text{nm}$ for $n = 100$ measurements) while long flexible fibers (heights $2.7 \pm 0.9\ \text{nm}$ for $n = 100$ measurements) were observed in the fibril preparations. ThT binding and fluorescence levels were significantly higher in the solutions containing fibrils compared to those containing oligomers (Figure 1B). This was consistent with the general understanding of fibrils as they are expected to have increased β -sheet character and a higher number of ThT binding sites. However, the observation that the oligomer preparations exhibited a considerable level of ThT fluorescence was somewhat surprising and suggested a significant level of β -structure.

The $A\beta(1-42)$ oligomer and fibril preparations were evaluated for their ability to stimulate TNF α production by microglia. TNF α is an important product of the MyD88-dependent proinflammatory innate immune response³⁵ and is measurably increased in post-mortem AD brain sections,⁷ and microvessels³⁶ and cerebrospinal fluid³⁷ of clinically diagnosed AD patients. Although most studies show similar responses between BV-2 and primary microglia, concerns have been raised that in some cases immortalized BV-2 microglia may not fully model primary microglia³⁸ and caution should be exercised when interpreting BV-2 results until direct comparison with primary cells can be made.³⁹ Therefore, it has become commonplace to utilize both microglial cell types for experimental testing which was the case in these studies. A 6 h incubation of $15\ \mu\text{M}$ $A\beta(1-42)$ oligomers or fibrils with murine microglia revealed significant differences in TNF α production between the two $A\beta$ aggregation states (Figure 2). Similar trends of inflammatory activity were observed in both primary (Figure 2A) and BV-2 (Figure 2B) microglia. Despite the lesser ThT fluorescence, the $A\beta(1-42)$ solutions prepared and incubated in oligomer-forming conditions were markedly better at inducing TNF α from murine microglia consistent with previous findings in rat astrocytes.²⁵

Characterization of SEC-Isolated $A\beta(1-42)$ Protofibrils Prepared and Eluted in Supplemented F12. Regardless of the conditions used to study $A\beta(1-42)$ aggregation there is always a degree of polydispersity present in the solutions which likely include monomers, soluble aggregates of many sizes, and some fibril structures. In order to better define and characterize the soluble $A\beta(1-42)$ aggregation species, SEC was used for separation and purification. SEC has been used in numerous studies to separate protofibrils from monomeric $A\beta$.^{11,40} In this

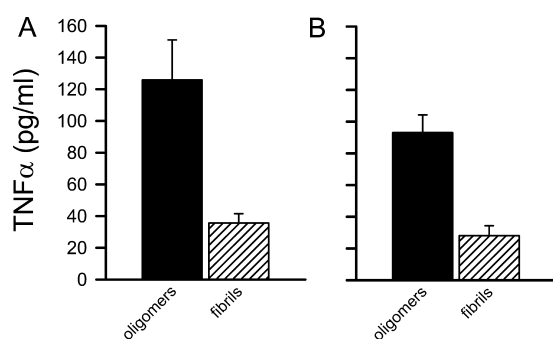


Figure 2. $A\beta(1-42)$ oligomers stimulate microglia more effectively than fibrils. Solutions of $A\beta(1-42)$ oligomers and fibrils prepared as in Figure 1 legend were incubated with microglia at a final concentration of $15 \mu\text{M}$ for 6 h. Secreted TNF α was measured by ELISA in the conditioned medium collected from treated primary murine microglia (panel A) and (panel B) BV-2 murine microglia. Data bars represent the average \pm standard (std) error of $n = 30$ trials (oligomers and fibrils) for primary microglia and $n = 32$ trials (oligomers) and $n = 33$ trials (fibrils) for BV-2 microglia. Control treatments in the presence of 0.3% DMSO in F-12 media or 1.5 mM HCl produced 40 and 15 pg/mL TNF α , respectively, for primary and BV-2 microglia and were subtracted from $A\beta$ -stimulated samples. Primary and BV-2 microglia were stimulated in serum-free and 2% FBS medium, respectively. Statistical differences between oligomers and fibrils for both sets of data had p values < 0.001 .

set of experiments, a Superdex 75 column was used for separation. Using a modified version of the NaOH method,⁴¹ lyophilized $A\beta(1-42)$ was reconstituted in NaOH followed by dilution in antibiotic-supplemented F-12 to prevent microbial growth. The use of F-12 media was retained from the oligomer-forming conditions in Figure 1 due to the physiological nature of the solution and the compatibility with microglial cell treatment. The $A\beta(1-42)$ solution ($250 \mu\text{M}$) was centrifuged at 18 000g and the supernatant was eluted in supplemented F-12 media as described in the Methods. The $A\beta(1-42)$ elution profile was monitored by UV absorbance (280 nm) and exhibited characteristic protofibril (void) and monomer (included) peaks (Figure 3).

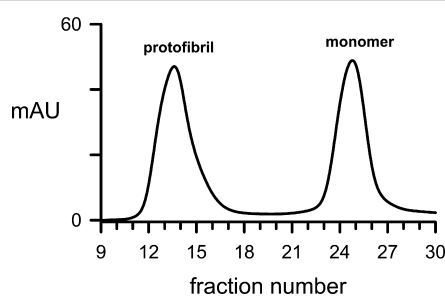


Figure 3. Dual peaks are observed following SEC elution of $A\beta(1-42)$ reconstituted in NaOH/F-12. Lyophilization $A\beta(1-42)$ (1 mg) was brought into solution with NaOH followed by supplemented F-12 media to a final concentration of $200 \mu\text{M}$. The supernatant after centrifugation was eluted from a Superdex 75 column, and 0.5 mL fractions were collected. UV absorbance at 280 nm was monitored during the elution (solid line).

The significant $A\beta(1-42)$ void peak was observed without prolonged incubation of the reconstitution solution confirming that $A\beta(1-42)$ forms protofibrils rapidly under these conditions.⁴²

SEC-purified monomer fractions did not exhibit ThT fluorescence while protofibril fractions at equivalent concentrations showed significant fluorescence (Figure 4A). Although

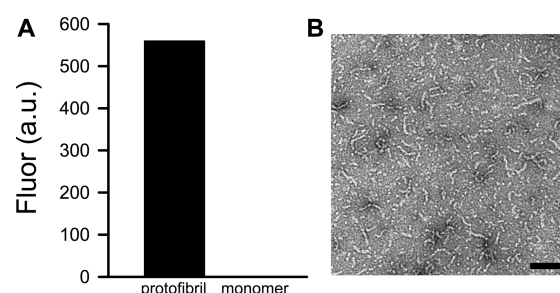


Figure 4. Structure and morphology of $A\beta(1-42)$ protofibrils. (A) Freshly isolated $A\beta(1-42)$ protofibrils and monomers after elution from Superdex 75 in supplemented F-12 were diluted to $5 \mu\text{M}$ respectively in supplemented F-12 containing $5 \mu\text{M}$ ThT, and fluorescence emission was measured as described in the Methods. (B) Protofibrils were diluted to $20 \mu\text{M}$, applied to a copper formvar grid, and imaged by TEM at a magnification of 43 000 \times . The scale bar represents 100 nm.

F-12 media is not a common Superdex 75 elution buffer such as Tris or PBS, transmission electron microscopy (TEM) imaging of the F-12-eluted void peak showed classic short curvilinear protofibrils^{11,43} < 100 nm in length (Figure 4B). Dynamic light scattering (DLS) measurements of the protofibril peak from seven separate SEC purifications produced an average R_H value of 21 nm with a standard deviation (std dev) of 6 nm (data not shown). Deconvolution of the average R_H values into histograms by data regularization revealed two predominant peaks of 4.5 ± 0.9 nm and 20.6 ± 6.5 nm. Peak 1 with the smaller R_H value was observed in 4 of 7 protofibril isolations, while peak 2 was always observed. Even within isolated $A\beta(1-42)$ protofibrils, a degree of polydispersity was present as the peak 2 histogram widths varied from narrow (e.g., 15–20 nm) to broad (e.g., 8–41 nm) in different experiments.

Microglial TNF α Production by SEC-Isolated $A\beta(1-42)$ Protofibrils, But Not Monomer. BV-2 murine microglia were treated with fresh SEC-isolated protofibril and monomer fractions and examined for their ability to stimulate an inflammatory response. Fraction concentrations were calculated based on UV absorbance and were used to determine final cellular treatment concentrations. Protofibrils ($15 \mu\text{M}$) induced a substantial level of secreted TNF α while monomers ($15 \mu\text{M}$) were much less effective (Figure 5). The presence of contaminating lipopolysaccharide (LPS) in SEC fractions was assessed in two ways, (1) a cell-free XTT assay in which the presence of any bacteria in the $A\beta$ samples would be expected to catalyze reduction of XTT and (2) TNF α production was monitored in the absence or presence of polymyxin B (PMX-B), a neutralizer of LPS signaling. The former method revealed no XTT reduction in the presence of $A\beta$ samples and in the latter method it was observed that PMX-B (100 ng/mL) had no effect on the $A\beta$ response yet blocked $>99\%$ of the LPS (3 ng/mL) response (data not shown). Thus, neither method showed any indication of bacterial or LPS presence. The findings demonstrated that isolated $A\beta(1-42)$ protofibrils were significant stimulators of BV-2 microglia whereas little stimulation was observed with purified monomeric $A\beta(1-42)$. The response to $A\beta(1-42)$ protofibrils was also tested in primary microglia isolated from newborn (3–4 day old) C57BL/6 mouse pups. Freshly isolated protofibrils were tested at multiple concentrations (5, 10, 15, and $20 \mu\text{M}$) and exhibited a dose-dependent ability to induce TNF α production in both primary and BV-2 microglia (Figure 6). Typically primary microglia were more responsive to $A\beta(1-42)$

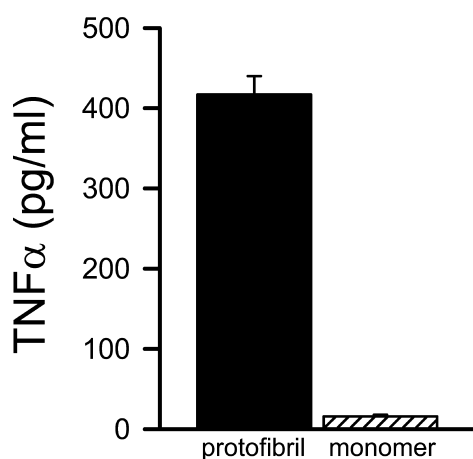


Figure 5. Protofibrils are significant stimulators of BV-2 microglia. SEC-isolated $A\beta(1-42)$ protofibrils and monomers in supplemented F-12 were incubated with BV-2 microglia at a final concentration of 15 μM for 6 h in medium containing 2% FBS. Secreted $\text{TNF}\alpha$ was measured by ELISA in the conditioned medium. Data bars represent the average \pm std error of $n = 6$ trials. Control treatments with an equal volume of supplemented F-12 media produced 23 pg/mL $\text{TNF}\alpha$ and were subtracted from $A\beta$ -stimulated samples.

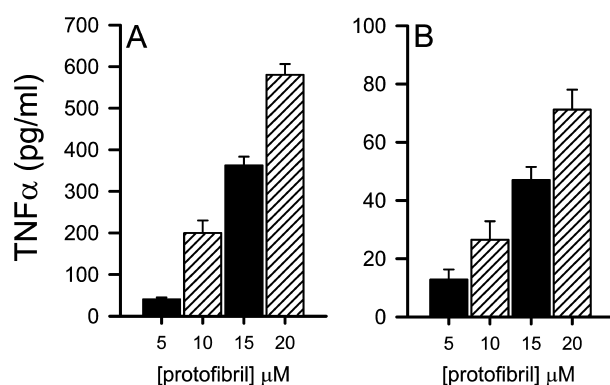


Figure 6. Protofibrils display a dose-dependent effect in their ability to induce $\text{TNF}\alpha$ production in microglia. SEC-isolated $A\beta(1-42)$ protofibrils in supplemented F-12 were incubated with primary microglia (panel A) or BV-2 microglia (panel B) for 6 h at final concentrations of 5, 10, 15, and 20 μM . Secreted $\text{TNF}\alpha$ was measured by ELISA in the conditioned medium. Data bars represent the average \pm std error of $n = 4-6$ trials at each concentration for primary microglia and $n = 6$ trials at each concentration for BV-2 microglia. Control treatments with supplemented F-12 media produced 6 and 17 pg/mL $\text{TNF}\alpha$ respectively for primary and BV-2 microglia and were subtracted from $A\beta$ -stimulated samples. Primary and BV-2 microglia were stimulated by $A\beta$ in serum-free conditions.

protofibrils than BV-2 microglia, but this disparity was dependent on the age and number of harvests of the primary cells as well as the BV-2 passage number. In some experiments, BV-2 cells secreted higher levels in response to $A\beta(1-42)$ protofibrils.

Comparison of Microglial $\text{TNF}\alpha$ Production between $A\beta(1-42)$ Protofibrils and Fibrils Prepared from SEC-Purified Monomer. We then sought to compare the microglial-activating ability of protofibrils and fibrils. SEC-purified $A\beta(1-42)$ monomer in supplemented F-12 was moved to 25 $^{\circ}\text{C}$ and subjected to gentle agitation for approximately 72 h. Fibrils were isolated by centrifugation, supernatant removal, and resuspension

of the pellet as described in the Methods. In all cases, >98% of the ThT fluorescence of the total solution was removed from the supernatant after centrifugation. ThT fluorescence comparisons of equivalent concentrations of $A\beta(1-42)$ fibrils and SEC-purified $A\beta(1-42)$ protofibrils and monomers immediately following elution showed fibrils with by far the best ThT binding ability (Figure 7A). Protofibrils displayed significantly lower ThT fluorescence and monomers were at background levels. TEM images of the isolated $A\beta(1-42)$ fibrils revealed long fibers with lengths exceeding 1 μm and typical widths of 5–10 nm (Figure 7B). The neutral pH and higher ionic strength of the F-12 media encouraged a considerable degree of lateral association between the fibrils. Surprisingly, fibrils were very poor in their ability to stimulate $\text{TNF}\alpha$ production in primary (Figure 7C) and BV-2 (data not shown) microglia. $A\beta(1-42)$ protofibrils invoked a dramatically higher microglial response compared to fibrils and monomers (Figure 7C). A cell-free XTT cell proliferation assay again showed no evidence of contamination in any of the preparations (data not shown). Our typical BV-2 and primary microglial preparations contained cells with both round and ramified morphologies with defined boundaries. After exposure to $A\beta$, the cells became clustered with rough boundaries and a less ramified morphology. These observations are consistent with those made by Garcao et al in rat microglia.⁴⁴ Primary microglia underwent more pronounced alterations in morphology compared to BV-2 cells. Even with these exterior changes to the cells after treatment with $A\beta$, no significant toxicity was observed using an XTT cell viability assay. Exposure of the microglia to $A\beta(1-42)$ fibrils, protofibrils, or monomer for 6 h did not inhibit mitochondrial-mediated reduction of XTT in either BV-2 or primary microglia (data not shown). The preparation of $A\beta$ protofibrils, fibrils, and monomers in the supplemented F-12, which is similar in pH and ionic strength to the microglial cell culture medium, likely helped prevent dramatic structural changes in the isolated $A\beta$ species when introduced to the microglia cells. Although this was not verified, very different microglial responses were clearly able to be observed between the distinct $A\beta$ species.

Comparison of Microglial $\text{TNF}\alpha$ Production between $A\beta(1-42)$ Protofibrils and $A\beta(1-40)$ Protofibrils. In order to compare $A\beta(1-40)$ protofibrils with those formed from $A\beta(1-42)$, a longer incubation was needed after NaOH reconstitution and dilution into supplemented F-12 medium. While $A\beta(1-42)$ protofibrils formed rapidly within minutes, $A\beta(1-40)$ required a 24 h incubation at 25 $^{\circ}\text{C}$ before significant amounts of protofibrils were generated (Figure 8). The $A\beta(1-40)$ protofibril fraction was assessed by TEM which revealed similar structures as observed for $A\beta(1-42)$ although the lengths appeared somewhat smaller (Figure 9A). Manual measurements of the images confirmed that the $A\beta(1-40)$ and $A\beta(1-42)$ protofibril fractions had statistically different ($p < 0.001$) lengths as $A\beta(1-40)$ protofibrils averaged 27 ± 11 nm while $A\beta(1-42)$ protofibrils averaged 50 ± 16 nm for $n = 50$ measurements. The length analysis only included unambiguous protofibril structures and excluded the smaller species (<15 nm). Despite morphological similarities, cellular studies demonstrated that $A\beta(1-40)$ protofibrils were much less effective in stimulating $\text{TNF}\alpha$ in primary microglia compared to $A\beta(1-42)$ protofibrils (Figure 9B). The concentration used in the microglial treatment for both $A\beta(1-40)$ and $A\beta(1-42)$ protofibrils was 15 μM .

The current report demonstrates the substantial activation of murine microglia by soluble $A\beta(1-42)$ aggregates. We observed

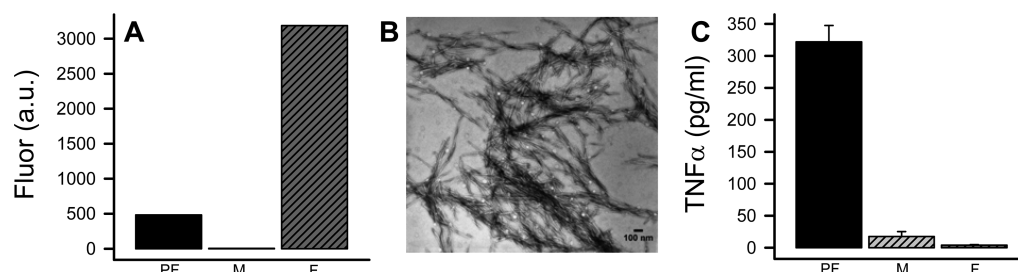


Figure 7. Protofibrils display less ThT fluorescence but stimulate microglia more effectively than fibrils. (A) Aliquots of SEC-purified Aβ(1-42) protofibrils (PF), monomer (M), and Aβ(1-42) fibrils formed from purified monomer (F) were diluted to 5 μM in 50 mM Tris-HCl pH 8.0 containing 5 μM ThT and fluorescence emission was measured and plotted as described in the Methods. Fibrils were isolated as described after gentle agitation for 72 h at 25 °C. One fluorescence measurement was obtained from each solution. (B) TEM images of isolated Aβ(1-42) fibril pellets (74 μM) at a magnification of 25,000. (C) Aliquots of the solutions described in panel (A) were incubated with primary murine microglia for 6 h at a final concentration of 15 μM Aβ(1-42). Secreted TNFα was measured by ELISA in the conditioned medium. Error bars represent the average ± std error of $n = 6$. Control treatments with supplemented F-12 media produced 15 pg/mL TNFα for primary microglia and were subtracted from Aβ-stimulated samples.

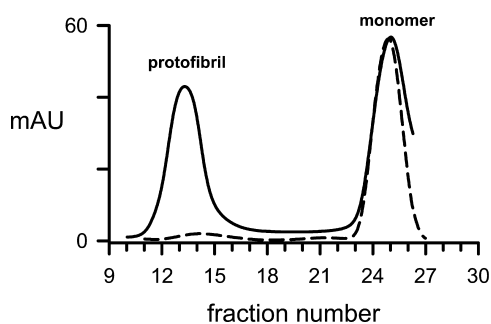


Figure 8. Aβ(1-40) protofibrils require longer incubation for formation. Aβ(1-40) was reconstituted and prepared for SEC as described in the Methods. Aβ(1-40) solutions were eluted on Superdex 75 immediately (dashed line) or after a 24 h incubation at 25 °C (solid line). Fractions containing protofibrils and monomers were immediately placed on ice for further characterization. Concentrations were determined by UV absorbance.

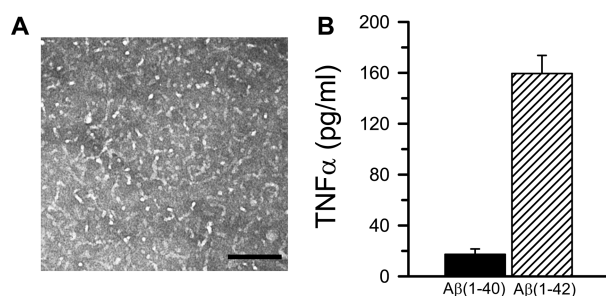


Figure 9. Aβ(1-40) protofibrils do not stimulate microglia as well as Aβ(1-42) protofibrils. (A) TEM image of a sample taken from the Aβ(1-40) protofibril peak in Figure 8 (solid line). Sample was diluted to 20 μM Aβ, applied to a copper formwar grid as described in the Methods, and imaged at a magnification of 43 000×. The scale bar represents 100 nm. (B) Primary microglia were incubated with Aβ(1-40) or Aβ(1-42) protofibrils isolated by SEC in supplemented F-12 at a final concentration of 15 μM each for 6 h. Secreted TNFα was measured by ELISA in the conditioned medium. Data bars represent the average ± std error of $n = 12$ (Aβ40) and $n = 9$ (Aβ42) trials over two separate protofibril preparations for each protofibril type. Protofibrils were directly compared within each cell treatment experiment. Control treatments with an equal volume of supplemented F-12 media produced 31 pg/mL TNFα and were subtracted from Aβ-stimulated samples.

that an enriched fraction of SEC-isolated protofibrils elicited the greatest production of the proinflammatory cytokine TNFα compared to monomers and fibrils. The current results have similarities to our previous findings in THP-1 human monocytes in which soluble fibrillar precursors were optimal for inducing a proinflammatory response.²⁶ While many studies have shown that monocytes and microglia have similar responses to Aβ, microglial cells provide a more relevant model system for investigating Aβ neuroinflammatory mechanisms. Furthermore, this report is the first to provide a direct comparison between SEC-purified Aβ(1-42) protofibrils and isolated Aβ(1-42) fibrils prepared from SEC-purified monomer in their ability to induce microglial activation.

An array of Aβ aggregate morphologies ranging from dense core neuritic plaques to granular diffuse wispy Aβ deposits are observed in the AD brain.¹ It has been known for some time that the plaques serve as a focal point for inflammation.⁵ The rapid response of microglia to a site of new plaque formation has been revealed using multiphoton microscopy in a transgenic mouse model outfitted with a cranial window.⁶ In this case, as well as others, microglia were not associated with diffuse Aβ deposits. Although it is not a straightforward extrapolation from in vitro results to in vivo mechanisms, the findings from our current study may be relevant to recent findings in transgenic mouse models. Hyman and colleagues observed a halo of oligomeric Aβ surrounding Aβ plaques based on immunostaining with NAB61 antibody.¹⁸ Although the plaques contain fibrillar Aβ at the core,⁴⁵ these data suggest that the plaque composition is more complex than originally thought. There may be dynamic aggregation processes occurring in the plaque environment and the microglial cells may interact with multiple Aβ species.

Much of the recent emphasis on soluble Aβ aggregates has been on oligomers yet much more structural information is known about protofibrils. The first observation and characterization of protofibrils more than a decade ago identified these small soluble species with significant β-sheet structure¹³ as precursors to fibrils.^{10,11} Centrifugation followed by SEC on Superdex 75 was instrumental in isolating protofibrils for further characterization.¹¹ Previous size analysis of protofibrils identified a range of R_H values from 10 to 50 nm and lengths of typically <200 nm.¹¹ The Aβ(1-42) protofibrils characterized in the current study were within these ranges but on the smaller end. The observation of bimodal R_H peaks in protofibril DLS

regularization histograms suggests that further separation and characterization may be possible. Structurally, protofibrils have similarities to fibrils based on thioflavin T binding, circular dichroism,¹³ and hydrogen exchange,⁴³ but have not yet developed the full stability of fibrillar $A\beta$.^{13,43} Protofibril diameters are typically smaller than fibrils and range from 4 to 6 nm although the protofibril to fibril transition can occur without a change in diameter.¹⁰ The transition to fibrils can occur via mechanisms that incorporate monomer deposition on protofibril ends, end-to-end annealing of protofibrils, and lateral association of protofibrils.^{12,34} Protofibrils display toxicity to neurons,¹³ disrupt ion channels,⁴⁶ inhibit hippocampal long-term potentiation,⁴⁷ and are likely to possess other detrimental biological activities. Their solubility and diffusible nature quite possibly render them more effective in cellular interactions and engaging microglial receptors compared to mature insoluble fibrils.

The mechanism by which $A\beta$ fibrils evoke a proinflammatory response appears to involve multiple cell-surface receptors. A multireceptor complex comprising the SR-B receptor CD36, $\alpha\beta_1$ -integrin, and the integrin-associated protein CD47 has been shown to mediate fibrillar $A\beta$ initiation of murine microglial activation.⁴⁸ Furthermore, receptor components of the innate immune system including CD14,⁴⁹ toll-like receptor (TLR) 2, and TLR 4 have also been identified as proinflammatory-linked receptors in microglial cells for $A\beta$ fibrils.³¹ Moreover, a TLR4-TLR6-CD36 complex was recently shown to mediate cellular inflammatory responses to $A\beta(1-42)$ fibrils.⁵⁰ A cell-surface receptor that is selective for $A\beta$ protofibrils has not been identified although the known fibril receptors may recognize similar structural elements between the two species.

For many years, it has been accepted that fibrillar $A\beta$ is the primary trigger for inducing a glial inflammatory response in AD and in cell culture models. Many studies established and utilized solution conditions that were optimal for $A\beta$ fibril formation but may have contained other $A\beta$ species. Nevertheless, it was generally interpreted as microglial activation by $A\beta$ fibrils. Numerous studies have demonstrated cytokine production by fibrillar $A\beta$,^{30,51} interaction of fibrillar $A\beta$ with proinflammatory receptors,⁴⁸⁻⁵⁰ and initiation of proinflammatory signaling pathways by fibrillar $A\beta$.^{52,53} More recently, studies have shown that a fibrillar state for $A\beta$ may not be required for microglial activation. These findings have been based on a lack of correlation between ThT binding and cell stimulation⁵⁴ or modulation of aggregation solution conditions to encourage formation of oligomers that display significant proinflammatory activity in microglia.^{24,25} A recent study altered the $A\beta$ aggregation solution conditions to encourage formation of smaller or larger oligomers and fibrils. Stimulation of primary mouse microglia with these solutions revealed that, while polydisperse in $A\beta$ species, those solutions containing smaller oligomers were able to induce more TNF α mRNA than those containing larger oligomers and fibrils.⁵⁵ Less has been published regarding $A\beta$ protofibrils and their role in AD-linked inflammation. In one study, Parvathy et al. found that $A\beta$ protofibrils were not effective at inducing IL-1 α mRNA expression in primary murine microglia compared to oligomers and fibrils.⁵⁶ This finding indicates that perhaps not all microglial proinflammatory products are upregulated to the same extent by $A\beta$ protofibrils. Interestingly, a new report suggests that soluble $A\beta$ aggregates may be one of the targets of the central nervous system glial cell response which includes both microglia and astrocytes. DaRocha-Souto et al. demonstrated in double-transgenic APP^{sw}-tau^{vhv} mice that the correlation between oligomeric $A\beta$ burden in the brain

(based on NAB61 antibody binding) and the number of reactive astrocytes was better than the correlation between total $A\beta$ plaque burden and reactive astrocytes.⁵⁷

Given the polydispersity observed in $A\beta$ aggregation, there is a good possibility that many preparations are not homogeneous. In fact, many studies focusing on a particular biological activity of $A\beta$ utilize $A\beta$ solutions that have not been rigorously characterized. These solutions likely contain mixtures of $A\beta$ aggregated species including oligomers, protofibrils, and fibrils. The conditions can dictate which species is more highly populated, but the mixture prevents the identification of the most active species. In fact, the $A\beta(1-42)$ solutions prepared in fibril-forming conditions (Figures 1 and 2) may have contained a small population of protofibrils which might help to explain why a moderate amount of microglial TNF α production was observed. The formation of these fibrils at very low ionic strength precluded the ability to utilize centrifugation to separate the fibrils from any contaminating protofibrils. However, the $A\beta(1-42)$ fibrils prepared from SEC-purified monomer at physiological pH and ionic strength (Figure 7) were very poor at stimulating TNF α production from microglia. This observation was possible due to the additional isolation step whereby fibrils were separated from the remaining $A\beta$ solution by centrifugation and resuspended before application to the cells. This procedure likely removed any soluble aggregated species that may have been present in the initial solution thus allowing isolated fibrils to be evaluated. Looking back on previous studies, the persistent use of $A\beta$ solutions containing a polydisperse population of aggregated species when evaluating $A\beta$ biological activity may help to explain significant fluctuations in cell response and irreproducibility between experiments. Furthermore, the $A\beta(1-42)$ fibrils described in Figures 1 and 2 were prepared under nonphysiological solution conditions (e.g., 10 mM HCl), and while the acidic conditions may have enhanced fibril formation, the internal structure may be quite different from the fibrils formed under more physiological conditions in Figure 7. Petkova et al. found that parallel β -sheet $A\beta(1-40)$ fibrils prepared under different conditions had distinct hydrogen-bond registries and marked differences in neuronal toxicity.⁵⁸ The same phenomenon has been observed for soluble aggregates. Chiti and co-workers demonstrated that oligomers grown under different solution conditions can have identical morphologies yet show different internal structures and toxicities.⁵⁹ There remain potential concerns with in vitro preparation of aggregated $A\beta$ species for cellular studies as their structure may have important differences from those formed in vivo. In the current study, the preparation, isolation, and characterization of $A\beta(1-42)$ protofibrils under close to physiological conditions may help avoid some of the concerns. The significant and consistent microglial response to an enriched SEC fraction of $A\beta(1-42)$ protofibrils demonstrates that these soluble fibrillar precursors are potent proinflammatory mediators. The much weaker microglial response to an equal concentration of $A\beta(1-40)$ protofibrils suggests that even though the two protofibril species appear morphologically similar, there are distinct properties between the two types of protofibrils that influence their inflammatory activity.

METHODS

Cell Culture and Primary Microglia Isolation. BV-2 cells are primary mouse microglial cells immortalized by stable transfection with the c-myc oncogene²⁷ and are functionally identical to native primary microglia.²⁸ BV-2 cells were provided by Dr. Gary Landreth,

Case Western Reserve University, and were maintained in Dulbecco's modified Eagle's medium (DMEM, 4.5 g/L glucose) (Hyclone) containing 50 U/mL penicillin, 50 μ g/mL streptomycin, 50 μ M β -mercaptoethanol, and 5% fetal bovine serum (FBS, Hyclone). BV-2 cells were used for their ease of culture, initial observations, optimization of microglia/ $A\beta$ interactions, and to reduce the usage of mice for primary cells. Primary murine microglia were obtained from newborn C57BL/6 mouse pups as previously described.²⁹ Care and breeding of the C57BL/6 parent mice (Harlan Laboratories) was done at the University of Missouri—St. Louis Animal Facility. Briefly, 3–4 day old mouse pups were euthanized with an overdose of inhaled isoflurane (Fisher Scientific). The brains were isolated and meninges were removed under sterile conditions. Brain tissue was minced using sharp edged forceps, resuspended in 0.5% trypsin (Hyclone), and incubated at 37 °C for 20 min to allow further dissociation of the tissue. Subsequently, tissue was resuspended in complete DMEM containing 10% fetal bovine serum, 4 mM L-glutamine, 100 U/mL penicillin, 0.1 mg/mL streptomycin and 0.25 μ g/mL amphotericin-B (Fisher Scientific), OPI medium supplement (oxalacetate, pyruvate, insulin, Sigma-Aldrich), and 0.5 ng/mL recombinant mouse granulocyte-macrophage colony-stimulating factor (GM-CSF) (Invitrogen). The cell suspension was further triturated using a pipet and filtered through a 70 μ m cell strainer to remove debris. The resulting cell suspension was centrifuged at 200g for 5 min at 25 °C, resuspended in complete medium, and seeded into 150 cm² flasks (Corning). Cells were cultured at 37 °C in 5% CO₂ until confluent (1–2 weeks), and microglia were selectively harvested from the adherent astrocyte layer by overnight shaking of the flask at 37 °C in 5% CO₂ and collection of the medium. The flasks were replenished with fresh medium and then incubated further to obtain additional microglia. Typically, this procedure was repeated 3–4 times for one flask without removal of the astrocyte layer.

Cell Stimulation Assay. For cellular studies, BV-2 microglia were removed from culture flasks with 0.25% trypsin and seeded in a sterile 96-well cell culture plate overnight at a density of 5×10^5 cells/mL in growth medium described above. Prior to cell treatment, medium was replaced with fresh medium containing either 0 or 2% FBS followed by $A\beta$ stimulation at a final concentration of 15 μ M. The inclusion of 2% FBS initially was adapted from an established THP-1 monocyte protocol.³⁰ Treatment of BV-2 without serum has been reported elsewhere³¹ and the absence of serum during BV-2 cell stimulation did not dramatically alter the results. The cells were incubated at 37 °C for 6 h in 5% CO₂, and the medium was collected and stored at –20 °C for subsequent analysis by enzyme-linked immunosorbent assay (ELISA). Primary microglia were collected after shaking flasks overnight and then centrifuged at 200g for 10 min at 25 °C. The cells were resuspended in complete microglial medium without GM-CSF or FBS and plated at a density of 5×10^5 cells/ml in a sterile 96-well cell culture plate for either 2 h or overnight. The longer preincubation, which has been used previously³¹ and was done to allow greater adherence of the microglia, had no deleterious effects on the cells. Prior to treatment, the medium was replaced again and lipopolysaccharide (3 ng/mL) or $A\beta$ (15 μ M) was added to the cells. The medium was collected after 6 h and stored at –20 °C for subsequent determination of secreted TNF α levels by ELISA. The background cellular response was assessed using the particular buffer vehicle for the $A\beta$.

ELISA. Measurement of secreted TNF α in the supernatants was determined by ELISA as previously detailed.³² Briefly, 96-well plates were coated overnight with monoclonal antimouse TNF α capture antibody, washed with phosphate-buffered saline (PBS) containing 0.05% Tween-20, and blocked with PBS containing 1% BSA, 5% sucrose, and 0.05% NaN₃ following by a wash step. Successive treatments with washing in between were done with samples or standards, biotinylated polyclonal antimouse TNF α detection antibody in 20 mM Tris with 150 mM NaCl and 0.1% BSA, streptavidin-horseradish peroxidase (HRP) conjugate, and equal volumes of HRP substrates 3,3',5,5'-tetramethylbenzidine and hydrogen peroxide. The reaction was stopped by the addition of 1% H₂SO₄ solution. The optical density of each sample was analyzed at 450 nm with a reference reading at 630 nm using a SpectraMax 340 absorbance plate reader (Molecular Devices, Union City, CA). The concentration of TNF α in the

experimental samples was calculated from a mouse TNF α standard curve of 15–2000 pg/mL. When necessary, samples were diluted to fall within the standard curve. TNF α concentrations for absorbance values below the lowest 15 pg/mL standard were determined by extrapolation of the standard curve regression line.

Preparation of $A\beta$ Peptides. $A\beta$ (1–42) was obtained from W.M. Keck Biotechnology Resource Laboratory (Yale School of Medicine, New Haven, CT) in lyophilized form and stored at –20 °C. $A\beta$ (1–40) was obtained from rPeptide (Bogarth, GA) or prepared by solid phase synthesis in the Structural Biology Core at the University of Missouri—Columbia as described previously.³³ $A\beta$ peptides were typically dissolved in 100% hexafluoroisopropanol (HFIP) (Sigma-Aldrich, St. Louis, MO) at 1 mM, aliquoted into sterile microcentrifuge tubes, and evaporated uncovered at room temperature overnight in a fume hood. The following day, the aliquots were vacuum-centrifuged to remove any residual HFIP and stored in desiccant at –20 °C. Some $A\beta$ peptides were treated with 100% trifluoroacetic acid and vacuum-centrifuged prior to HFIP treatment. $A\beta$ oligomers and fibrils obtained directly from lyophilized aliquots were prepared as previously described.¹⁴ Briefly, lyophilized $A\beta$ 42 aliquots were resuspended in sterile anhydrous dimethyl sulfoxide (DMSO) (Sigma-Aldrich, St. Louis, MO) at 5 mM. For oligomer preparation the sample was diluted to 100 μ M in sterile ice-cold Ham's F-12 cell culture medium with L-glutamine but without phenol red (F-12, Bioworld, Dublin, OH) and incubated for 24 h at 4 °C. For fibril preparation, the sample was diluted to 100 μ M in 10 mM HCl and incubated for 24 h at 37 °C. $A\beta$ concentrations in these preparations were based on dry peptide weight.

Size Exclusion Chromatography. An amount of 1–1.5 mg of lyophilized $A\beta$ peptide was dissolved in 50 mM NaOH to yield a 2.5 mM $A\beta$ solution. The solution was then diluted to 250 μ M $A\beta$ in sterile prefiltered (0.22 μ m) Ham's F-12 cell culture medium (described above) with additional supplementation of 100 U/mL penicillin, 0.1 mg/mL streptomycin, and 0.25 μ g/mL amphotericin-B (heretofore referred to as supplemented F-12). $A\beta$ (1–42) solutions were centrifuged immediately at 18 000g for 10 min with a Beckman-Coulter Microfuge18 instrument while $A\beta$ (1–40) solutions were incubated for 24 h at 25 °C prior to size-exclusion chromatography (SEC). The centrifugation supernatant was eluted from a Superdex 75 HR 10/30 column (GE Healthcare) in supplemented F-12 medium. Prior to injection of $A\beta$, Superdex 75 column was coated with 2 mg bovine serum albumin (BSA, Sigma) to prevent any nonspecific binding of $A\beta$ to the column matrix. Following a 1 mL loading of the sample, $A\beta$ was eluted at 0.5 mL/min and 0.5 mL fractions were collected and immediately placed on ice. Fractions 13, 14 eluting in the void volume were pooled together and designated as protofibrils while fractions 24–25 eluting in the included peak were pooled and designated as monomer. UV absorbance at 280 nm was monitored continuously in milliabsorbance units (mAU) during the elution, and concentrations of both protofibrils and monomers were determined directly from the absorbance trace using an extinction coefficient of 1450 cm^{–1} M^{–1} at 280 nm. The delay volume between the absorbance detector and fraction collector was minimal, and this was verified in initial experiments by measuring $A\beta$ concentrations in the fractions on a Cary Bio 50 UV absorbance spectrophotometer and comparing those concentration values to those determined from the chromatography absorbance trace. $A\beta$ (1–42) fibrils were prepared from SEC-purified $A\beta$ (1–42) monomer in supplemented F-12 by incubation at room temperature under gentle agitation for ~72 h. The aggregated $A\beta$ (1–42) solution was then centrifuged at 18 000g for 10 min, supernatant was removed, and the pellet was resuspended in the same volume of supplemented F-12. The concentration of fibrils was assumed to match the original starting concentration of the $A\beta$ (1–42) monomer. Thioflavin-T (ThT) fluorescence measurements were done on the total $A\beta$ (1–42) solution, the 18 000 g supernatant, and the resuspended pellet in order to monitor the conversion of $A\beta$ monomer into fibrils.

Thioflavin T Fluorescence Measurements. $A\beta$ (1–42) monomer, protofibril and fibril solutions were assessed by ThT fluorescence as described previously.³⁴ $A\beta$ aliquots were removed and diluted 10-fold into 50 mM Tris-HCl pH 8.0 containing 5 μ M ThT. Fluorescence

emission scans (460–520 nm) were acquired on a Cary Eclipse fluorescence spectrophotometer using an excitation wavelength of 450 nm and integrated from 470 to 500 nm to obtain ThT relative fluorescence values. F-12 medium, supplemented or not, did not show any significant ThT fluorescence in the absence of A β . All ThT fluorescence numbers are reported in relative fluorescence units denoted arbitrary units (a.u.) in the figures.

Atomic Force Microscopy. A β (1–42) aggregation solutions (100 μ M) were diluted to 10 μ M in water. Grade V1 mica (Ted Pella, Inc., Redding, CA) was cut into 11 mm circles and affixed to 12 mm metal discs. Aliquots (50 μ L) were applied to freshly cleaved mica, allowed to adsorb for 15 min, washed twice with water, air-dried, and stored in a container with desiccant. Images were obtained with a Nanoscope III multimode atomic force microscope (Digital Instruments, Santa Barbara, CA) in TappingMode. Height analysis was performed using Nanoscope III software on flattened height mode images.

Transmission Electron Microscopy. SEC-purified A β (1–42) protofibril and aggregation solutions were diluted to 20 μ mol/L in water unless otherwise stated and applied (10 μ L) to a 200-mesh Formvar-coated copper grid (Ted Pella, Inc.). Samples were allowed to adsorb for 10 min at 25 °C, followed by removal of excess sample solution. Grids were washed three times by placing the sample side down on a droplet of water. Heavy metal staining was done by incubation of the grid on a droplet of 2% uranyl acetate (Electron Microscopy Sciences, Hatfield, PA) for 5 min, removal of excess solution, and air drying. Affixed samples were visualized with a JEOL JEM-2000 FX transmission electron microscope operated at 200k eV.

Dynamic Light Scattering. Hydrodynamic radius (R_H) measurements were made at room temperature with a DynaPro Titan instrument (Wyatt Technology, Santa Barbara, CA). Samples (30 μ L) were placed directly into a quartz cuvette and light scattering intensity was collected at a 90° angle using a 10 s acquisition time. Particle diffusion coefficients were calculated from autocorrelated light intensity data and converted to R_H with the Stokes–Einstein equation. Average R_H values were obtained with Dynamics software (version 6.7.1). Histograms of percent intensity vs R_H were generated by Dynamics data regularization and intensity-weighted mean R_H values were derived from the regularized histograms.

XTT Cell Viability and Proliferation Assay. Viability of A β -treated microglia was determined by using an XTT [2, 3-bis (2-methoxy-4-nitro-5-sulfophenyl)-2H-tetrazolium-5-carboxanilide] assay. Cellular metabolic activity was monitored by mitochondria-mediated reduction of XTT (Sigma). XTT assay was also used in a cell-free manner to rule out the possibility of any bacterial contamination of A β (1–42) and A β (1–40) samples. In cellular XTT assay, cells exposed to A β for 6 h were further incubated with 0.33 mg/mL XTT and 8.3 μ M phenazine methosulfate (PMS) (Acros, Morris Plains, NJ) for 2 h at 37 °C. The extent of XTT reduction was measured by absorbance of reduced form of XTT at 467 nm. The cell-free XTT assay was done in parallel to the cell stimulation studies, in a similar manner as above except the A β sample was incubated with XTT and PMS without any cells at the same final concentration of 15 μ M for 6 h.

Statistical Analysis. Cellular responses and protofibril length measurements were evaluated for statistical differences by paired *t* test analysis in SigmaPlot 10.0 software.

AUTHOR INFORMATION

Corresponding Author

*Mailing address: Department of Chemistry and Biochemistry, University of Missouri—St. Louis, One University Boulevard, St. Louis, Missouri 63121. Telephone: (314) 516-7345. Fax: (314) 516-5342. E-mail: nicholsmic@umsl.edu.

Author Contributions

M.N. conceived the project. G.P. performed the following: preparation and purification of protofibril, monomer, and fibril samples, cell culture and primary microglia isolation, microglial activation studies, toxicity assays, ELISA, and fluorescence

measurements. L.G. did the AFM imaging and analysis. D.O. did the TEM imaging. M.N. performed the DLS studies. M.N. and G.P. wrote the paper.

Funding

This work was supported by Award Number R15AG033913 from the National Institute on Aging (M.R.N.).

Notes

The authors declare no competing financial interest.

ACKNOWLEDGMENTS

We would like to thank Dr. Tammy L. Kielian and Ms. Teresa Fritz at the University of Nebraska Medical Center for training and advice in primary murine microglia isolation and the Microscopy Image and Spectroscopy Technology Laboratory in the Center for Nanoscience at University of Missouri—St. Louis for technical assistance and equipment.

ABBREVIATIONS

AD, Alzheimer's disease; A β , amyloid- β protein; HFIP, hexafluoroisopropanol; SEC, size exclusion chromatography; ThT, thioflavin T; TEM, transmission electron microscopy; AFM, atomic force microscopy; DLS, dynamic light scattering

REFERENCES

- (1) Selkoe, D. J. (2004) Cell biology of protein misfolding: The examples of Alzheimer's and Parkinson's diseases. *Nat. Cell Biol.* 6, 1054–1061.
- (2) Fagan, A. M., and Holtzman, D. M. (2010) Cerebrospinal fluid biomarkers of Alzheimer's disease. *Biomarkers Med.* 4, 51–63.
- (3) Suzuki, N., Cheung, T. T., Cai, X. D., Odaka, A., Otvos, L. Jr., Eckman, C., Golde, T. E., and Younkin, S. G. (1994) An increased percentage of long amyloid β protein secreted by familial amyloid β protein precursor (β APP₇₁₇) mutants. *Science* 264, 1336–1340.
- (4) Haass, C., and Selkoe, D. J. (2007) Soluble protein oligomers in neurodegeneration: lessons from the Alzheimer's amyloid β -peptide. *Nat. Rev. Mol. Cell Biol.* 8, 101–112.
- (5) McGeer, P. L., Itagaki, S., Tago, H., and McGeer, E. G. (1987) Reactive microglia in patients with senile dementia of the Alzheimer type are positive for the histocompatibility glycoprotein HLA-DR. *Neurosci. Lett.* 79, 195–200.
- (6) Meyer-Luehmann, M., Spires-Jones, T. L., Prada, C., Garcia-Alloza, M., de Calignon, A., Rozkalne, A., Koenigsknecht-Talboo, J., Holtzman, D. M., Bacskai, B. J., and Hyman, B. T. (2008) Rapid appearance and local toxicity of amyloid- β plaques in a mouse model of Alzheimer's disease. *Nature* 451, 720–724.
- (7) Dickson, D. W., Lee, S. C., Mattiace, L. A., Yen, S. H. C., and Brosnan, C. (1993) Microglia and cytokines in neurological disease, with special reference to AIDS and Alzheimer disease. *Glia* 7, 75–83.
- (8) McGeer, E. G., and McGeer, P. L. (1998) The importance of inflammatory mechanisms in Alzheimer disease. *Exp. Gerontol.* 33, 371–378.
- (9) Golde, T. E. (2002) Inflammation takes on Alzheimer disease. *Nat. Med.* 8, 936–938.
- (10) Harper, J. D., Wong, S. S., Lieber, C. M., and Lansbury, P. T. Jr. (1997) Observation of metastable A β amyloid protofibrils by atomic force microscopy. *Chem. Biol.* 4, 119–125.
- (11) Walsh, D. M., Lomakin, A., Benedek, G. B., Condron, M. M., and Teplow, D. B. (1997) Amyloid β -protein fibrillogenesis: Detection of a protofibrillar intermediate. *J. Biol. Chem.* 272, 22364–22372.
- (12) Harper, J. D., Wong, S. S., Lieber, C. M., and Lansbury, P. T. Jr. (1999) Assembly of A β amyloid peptides: an *in vitro* model for a possible early event in Alzheimer's disease. *Biochemistry* 38, 8972–8980.
- (13) Walsh, D. M., Hartley, D. M., Kusumoto, Y., Fezoui, Y., Condron, M. M., Lomakin, A., Benedek, G. B., Selkoe, D. J., and Teplow, D. B. (1999) Amyloid β -protein fibrillogenesis: Structure and

biological activity of protofibrillar intermediates. *J. Biol. Chem.* 274, 25945–25952.

(14) Stine, W. B. J., Dahlgren, K. N., Krafft, G. A., and LaDu, M. J. (2003) *In vitro* characterization of conditions for amyloid- β peptide oligomerization and fibrillogenesis. *J. Biol. Chem.* 278, 11612–11622.

(15) Jarrett, J. T., Berger, E. P., and Lansbury, P. T. Jr. (1993) The carboxy terminus of the β amyloid protein is critical for the seeding of amyloid formation: Implications for the pathogenesis of Alzheimer's disease. *Biochemistry* 32, 4693–4697.

(16) Dahlgren, K. N., Manelli, A. M., Stine, W. B. Jr., Baker, L. K., Krafft, G. A., and LaDu, M. J. (2002) Oligomeric and fibrillar species of amyloid- β peptides differentially affect neuronal viability. *J. Biol. Chem.* 277, 32046–32053.

(17) Harper, J. D., Lieber, C. M., and Lansbury, P. T. Jr. (1997) Atomic force microscopic imaging of seeded fibril formation and fibril branching by the Alzheimer's disease amyloid- β protein. *Chem. Biol.* 4, 951–959.

(18) Koffie, R. M., Meyer-Luehmann, M., Hashimoto, T., Adams, K. W., Mielke, M. L., Garcia-Alloza, M., Micheva, K. D., Smith, S. J., Kim, M. L., Lee, V. M., Hyman, B. T., and Spire-Jones, T. L. (2009) Oligomeric amyloid β associates with postsynaptic densities and correlates with excitatory synapse loss near senile plaques. *Proc. Natl. Acad. Sci. U.S.A.* 106, 4012–4017.

(19) Deshpande, A., Mina, E., Glabe, C., and Busciglio, J. (2006) Different conformations of amyloid β induce neurotoxicity by distinct mechanisms in human cortical neurons. *J. Neurosci.* 26, 6011–6018.

(20) Lorenzo, A., and Yankner, B. A. (1994) β -amyloid neurotoxicity requires fibril formation and is inhibited by Congo red. *Proc. Natl. Acad. Sci. U.S.A.* 91, 12243–12247.

(21) Pike, C. J., Walencewicz, A. J., Glabe, C. G., and Cotman, C. W. (1991) *In vitro* aging of β -amyloid protein causes peptide aggregation and neurotoxicity. *Brain Res.* 563, 311–314.

(22) Walsh, D. M., Klyubin, I., Fadeeva, J. V., Cullen, W. K., Anwyl, R., Wolfe, M. S., Rowan, M. J., and Selkoe, D. J. (2002) Naturally secreted oligomers of amyloid β protein potently inhibit hippocampal long-term potentiation *in vivo*. *Nature* 416, 535–539.

(23) Heneka, M. T., and O'Banion, M. K. (2007) Inflammatory processes in Alzheimer's disease. *J. Neuroimmunology* 184, 69–91.

(24) Sondag, C. M., Dhawan, G., and Combs, C. K. (2009) Beta amyloid oligomers and fibrils stimulate differential activation of primary microglia. *J. Neuroinflammation* 6, 1.

(25) White, J. A., Manelli, A. M., Holmberg, K. H., Van Eldik, L. J., and Ladu, M. J. (2005) Differential effects of oligomeric and fibrillar amyloid- β 1–42 on astrocyte-mediated inflammation. *Neurobiol. Dis.* 18, 459–465.

(26) Ajit, D., Udan, M. L., Paranjape, G., and Nichols, M. R. (2009) Amyloid- β (1–42) fibrillar precursors are optimal for inducing tumor necrosis factor- α production in the THP-1 human monocytic cell line. *Biochemistry* 48, 9011–9021.

(27) Banati, R. B., and Graeber, M. B. (1994) Surveillance, intervention and cytotoxicity: is there a protective role of microglia? *Dev. Neurosci.* 16, 114–127.

(28) Lehrmann, E., Kiefer, R., Christensen, T., Toyka, K. V., Zimmer, J., Diemer, N. H., Hartung, H. P., and Finsen, B. (1998) Microglia and macrophages are major sources of locally produced transforming growth factor- β , after transient middle cerebral artery occlusion in rats. *Glia* 24, 437–448.

(29) Esen, N., and Kielian, T. (2007) Effects of low dose GM-CSF on microglial inflammatory profiles to diverse pathogen-associated molecular patterns (PAMPs). *J. Neuroinflammation* 4, 10.

(30) Yates, S. L., Burgess, L. H., Kocsis-Angle, J., Antal, J. M., Dority, M. D., Embury, P. B., Piotrkowski, A. M., and Brunden, K. R. (2000) Amyloid beta and amylin fibrils induce increases in proinflammatory cytokine and chemokine production by THP-1 cells and murine microglia. *J. Neurochem.* 74, 1017–1025.

(31) Reed-Geaghan, E. G., Savage, J. C., Hise, A. G., and Landreth, G. E. (2009) CD14 and Toll-like receptors 2 and 4 are required for fibrillar A β -stimulated microglial activation. *J. Neurosci.* 29, 11982–11992.

(32) Udan, M. L., Ajit, D., Crouse, N. R., and Nichols, M. R. (2008) Toll-like receptors 2 and 4 mediate A β (1–42) activation of the innate immune response in a human monocytic cell line. *J. Neurochem.* 104, 524–533.

(33) McDonough, R. T., Paranjape, G., Gallazzi, F., and Nichols, M. R. (2011) Substituted tryptophans at amyloid- β (1–40) residues 19 and 20 experience different environments after fibril formation. *Arch. Biochem. Biophys.* 514, 27–32.

(34) Nichols, M. R., Moss, M. A., Reed, D. K., Lin, W. L., Mukhopadhyay, R., Hoh, J. H., and Rosenberry, T. L. (2002) Growth of β -amyloid(1–40) protofibrils by monomer elongation and lateral association. Characterization of distinct products by light scattering and atomic force microscopy. *Biochemistry* 41, 6115–6127.

(35) Kielian, T. (2006) Toll-like receptors in central nervous system glial inflammation and homeostasis. *J. Neurosci. Res.* 83, 711–730.

(36) Grammas, P., and Ovase, R. (2001) Inflammatory factors are elevated in brain microvessels in Alzheimer's disease. *Neurobiol. Aging* 22, 837–842.

(37) Tarkowski, E., Andreasen, N., Tarkowski, A., and Blennow, K. (2003) Intrathecal inflammation precedes development of Alzheimer's disease. *J. Neurol., Neurosurg. Psychiatry* 74, 1200–1205.

(38) Horvath, R. J., Nutile-McMenemy, N., Alkatis, M. S., and DeLeo, J. A. (2008) Differential migration, LPS-induced cytokine, chemokine, and NO expression in immortalized BV-2 and HAPI cell lines and primary microglial cultures. *J. Neurochem.* 107, 557–569.

(39) Romero-Sandoval, E. A., Horvath, R., Landry, R. P., and DeLeo, J. A. (2009) Cannabinoid receptor type 2 activation induces a microglial anti-inflammatory phenotype and reduces migration via MKP induction and ERK dephosphorylation. *Mol. Pain* 5, 25.

(40) Jan, A., Hartley, D. M., and Lashuel, H. A. (2010) Preparation and characterization of toxic A β aggregates for structural and functional studies in Alzheimer's disease research. *Nat. Protoc.* 5, 1186–1209.

(41) Teplow, D. B. (2006) Preparation of amyloid β -protein for structural and functional studies. *Methods Enzymol.* 413, 20–33.

(42) Jan, A., Adolffson, O., Allaman, I., Buccarello, A. L., Magistretti, P. J., Pfeifer, A., Muhs, A., and Lashuel, H. A. (2011) A β 42 neurotoxicity is mediated by ongoing nucleated polymerization process rather than by discrete A β 42 species. *J. Biol. Chem.* 286, 8585–8596.

(43) Kheterpal, I., Lashuel, H. A., Hartley, D. M., Walz, T., Lansbury, P. T. Jr., and Wetzel, R. (2003) A β protofibrils possess a stable core structure resistant to hydrogen exchange. *Biochemistry* 42, 14092–14098.

(44) Garcao, P., Oliveira, C. R., and Agostinho, P. (2006) Comparative study of microglia activation induced by amyloid-beta and prion peptides: role in neurodegeneration. *J. Neurosci. Res.* 84, 182–93.

(45) Terry, R. D., Gonatas, N. K., and Weiss, M. (1964) Ultrastructural studies in Alzheimer's presenile dementia. *Am. J. Pathol.* 44, 269–297.

(46) Ye, C. P., Selkoe, D. J., and Hartley, D. M. (2003) Protofibrils of amyloid β -protein inhibit specific K⁺ currents in neocortical cultures. *Neurobiol. Dis.* 13, 177–190.

(47) O'Nuallain, B., Freir, D. B., Nicoll, A. J., Risse, E., Ferguson, N., Herron, C. E., Collinge, J., and Walsh, D. M. (2010) Amyloid β -protein dimers rapidly form stable synaptotoxic protofibrils. *J. Neurosci.* 30, 14411–14419.

(48) Bamberger, M. E., Harris, M. E., McDonald, D. R., Husemann, J., and Landreth, G. E. (2003) A cell surface receptor complex for fibrillar β -amyloid mediates microglial activation. *J. Neurosci.* 23, 2665–2674.

(49) Fassbender, K., Walter, S., Kuhl, S., Landmann, R., Ishii, K., Bertsch, T., Stalder, A. K., Muehlhauser, F., Liu, Y., Ulmer, A. J., Rivest, S., Lentschat, A., Gulbins, E., Jucker, M., Staufenbiel, M., Brechtel, K., Walter, J., Multhaup, G., Penke, B., Adachi, Y., Hartmann, T., and Beyreuther, K. (2004) The LPS receptor (CD14) links innate immunity with Alzheimer's disease. *FASEB J.* 18, 203–205.

(50) Stewart, C. R., Stuart, L. M., Wilkinson, K., van Gils, J. M., Deng, J., Halle, A., Rayner, K. J., Boyer, L., Zhong, R., Frazier, W. A., Lacy-Hulbert, A., Khoury, J. E., Golenbock, D. T., and Moore, K. J. (2010)

CD36 ligands promote sterile inflammation through assembly of a Toll-like receptor 4 and 6 heterodimer. *Nat. Immunol.* 11, 155–161.

(51) Meda, L., Cassatella, M. A., Szendrei, G. I., Otvos, L. Jr., Baron, P., Villalba, M., Ferrari, D., and Rossi, F. (1995) Activation of microglial cells by β -amyloid protein and interferon- γ . *Nature* 374, 647–50.

(52) McDonald, D. R., Bamberger, M. E., Combs, C. K., and Landreth, G. E. (1998) β -Amyloid fibrils activate parallel mitogen-activated protein kinase pathways in microglia and THP1 monocytes. *J. Neurosci.* 18, 4451–4460.

(53) Della Bianca, V., Dusi, S., Bianchini, E., Dal Pra, I., and Rossi, F. (1999) β -amyloid activates the O₂ forming NADPH oxidase in microglia, monocytes, and neutrophils - A possible inflammatory mechanism of neuronal damage in Alzheimer's disease. *J. Biol. Chem.* 274, 15493–15499.

(54) Hashioka, S., Monji, A., Ueda, T., Kanba, S., and Nakanishi, H. (2005) Amyloid- β fibril formation is not necessarily required for microglial activation by the peptides. *Neurochem. Int.* 47, 369–76.

(55) Heurtaux, T., Michelucci, A., Losciuto, S., Gallotti, C., Felten, P., Dorban, G., Grandbarbe, L., Morga, E., and Heuschling, P. (2010) Microglial activation depends on beta-amyloid conformation: role of the formylpeptide receptor 2. *J. Neurochem.* 114, 576–586.

(56) Parvathy, S., Rajadas, J., Ryan, H., Vaziri, S., Anderson, L., and Murphy, G. M. Jr. (2009) A β peptide conformation determines uptake and interleukin-1 α expression by primary microglial cells. *Neurobiol. Aging* 30, 1792–1804.

(57) DaRocha-Souto, B., Scotton, T. C., Coma, M., Serrano-Pozo, A., Hashimoto, T., Sereno, L., Rodriguez, M., Sanchez, B., Hyman, B. T., and Gomez-Isla, T. (2011) Brain oligomeric β -amyloid but not total amyloid plaque burden correlates with neuronal loss and astrocyte inflammatory response in amyloid precursor protein/tau transgenic mice. *J. Neuropathol. Exp. Neurol.* 70, 360–376.

(58) Petkova, A. T., Leapman, R. D., Guo, Z., Yau, W. M., Mattson, M. P., and Tycko, R. (2005) Self-propagating, molecular-level polymorphism in Alzheimer's β -amyloid fibrils. *Science* 307, 262–265.

(59) Campioni, S., Mannini, B., Zampagni, M., Pensalfini, A., Parrini, C., Evangelisti, E., Relini, A., Stefani, M., Dobson, C. M., Cecchi, C., and Chiti, F. (2010) A causative link between the structure of aberrant protein oligomers and their toxicity. *Nat. Chem. Biol.* 6, 140–147.